Scheduling with Predictable Link Reliability for Wireless Networked Control

Hongwei Zhang, Xiaohui Liu, Chuan Li,
Yu Chen, Xin Che, Le Yi Wang, Feng Lin, George Yin

Abstract

Predictable link reliability is required for wireless networked control, yet co-channel interference remains a major source of uncertainty in wireless link reliability. Formulated specifically for distributed, predictable control of co-channel interference, the physical-ratio-K (PRK) interference model integrates the protocol model's locality and the physical model's high fidelity while addressing their weaknesses, and it has the potential to enable scheduling with predictable link reliability. To realize the potential of the PRK model, we design protocol PRKS that addresses the challenges of model instantiation and protocol signaling in PRK-based scheduling. In particular, PRKS uses a control-theoretic approach to instantiate the PRK model, it uses local signal maps to address the challenges of large interference range and anisotropic, asymmetric wireless communication, and it leverages the different timescales of PRK model adaptation and data transmission to decouple protocol signaling from data transmission. Through testbed-based measurement study, we show that, unlike existing scheduling protocols where link reliability is unpredictable and the ratio of links whose reliability meets application requirements can be as low as 0%, PRKS enables predictably high link reliability (e.g., 95%) for all the links in different network and environmental conditions without a priori knowledge of these conditions. Through local, distributed coordination, PRKS also achieves a channel spatial reuse very close to what is enabled by the state-of-the-art centralized scheduler while ensuring the required link reliability. By ensuring the required link reliability in scheduling, PRKS also enables a lower communication delay and a higher network throughput than existing scheduling protocols.

I. Introduction

Embedded wireless networks are increasingly being explored for real-time control of physical processes such as those in industrial IoT systems [1], [2], [3]. In wireless networked control

The authors' work is supported in part by NSF awards CNS-1136007, CNS-1054634, and GENI-1890. An extended abstract containing some preliminary results of this paper appeared in IEEE/ACM IWQoS'15.

Hongwei Zhang, Xiaohui Liu, Chuan Li, Yu Chen, Xin Che, Feng Lin, and George Yin are with Wayne State University, U.S.A. E-mail: {ongwei,xiaohui,chuan,yu_chen,chexin,lywang,flin,gyin}@wayne.edu.

(WNC), communication across wireless networks is a basic enabler for the coordination among distributed sensors, controllers, and actuators; in supporting mission-critical tasks such as industrial process control, wireless communication is required to be reliable (i.e., having high delivery ratio) [2], [3]. Given the varying impact that the reliability, delay, and throughput of wireless communication have on networked control and the inherent tradeoff between communication reliability, delay, and throughput, the optimal operation of WNC systems requires controlling the tradeoff between the reliability, delay, and throughput in communication, where controlling data communication reliability across wireless links (or *link reliability* for short) in a predictable manner is a basis for such system-level optimization [2], [4], [5], [6]. Causing collisions of concurrent transmissions, co-channel interference is a major source of unpredictability in link reliability [6], [7], [8]. Thus scheduling transmissions for co-channel interference control is a basic element of wireless communication in WNC systems.

Distributed scheduling & PRK interference model. In WNC systems, not only do wireless link dynamics introduce uncertainty as in traditional wireless sensor networks, dynamic control strategies also introduce dynamic network traffic patterns and pose different requirements on communication reliability [4]. For agile adaptation to uncertainties and for avoiding information inconsistency in centralized scheduling, distributed scheduling becomes desirable for interference control in wireless control networks. Despite decades of research on interference-oriented channel access control, most existing literature are either based on the physical interference model or the protocol interference model, neither of which is a good foundation for distributed interference control in the presence of uncertainties [6], [9], [10], [11]. The physical model has high-fidelity, but it is non-local and combinatorial and thus not suitable for distributed protocol design in dynamic, uncertain settings; the protocol model is local and suitable for distributed protocol design, but it is inaccurate and does not ensure reliable data delivery in general [6], [12].

Without field-deployable solutions to predictable co-channel interference control, current systems practice, such as the WirelessHART standard for industrial sensing and control [13], avoids co-channel interference by allowing only one node in the whole network to transmit in a wireless channel at any moment in time. Without spatial channel reuse, however, this approach does not fully utilize wireless network capacity, which is undesirable for high data-rate control applications and for new networked control paradigms that involve communications between close-by nodes only [14].

To address the gap between the existing interference models and the design of distributed,

field-deployable scheduling protocols with predictable data delivery reliability, Zhang et al. [6] have recently identified the *physical-ratio-K (PRK) interference model that defines pairwise interference relations between close-by nodes only while ensuring application-required communication reliability*. In the PRK model, a node C' is regarded as not interfering and thus can transmit concurrently with the transmission from another node S to its receiver R if and only if $P(C', R) < \frac{P(S,R)}{K_{S,R,T_{S,R}}}$, where $P(C', R)$ and $P(S, R)$ is the average strength of signals reaching R from C' and S respectively, and $K_{S,R,T_{S,R}}$ is the minimum real number chosen such that, in the presence of background noise and cumulative interference from all concurrent transmitters in the network, the probability for R to successfully receive packets from S is no less than the minimum link reliability $T_{S,R}$ required by applications (e.g., control algorithms). As shown in Figure 1, the PRK model defines, for each link (S, R), an exclusion region $\mathbb{E}_{S,R,T_{S,R}}$ around the receiver R such that a node $C \in \mathbb{E}_{S,R,T_{S,R}}$ if and only if $P(C, R) \geq \frac{P(S,R)}{K_{S,R,T_{S,R}}}$. Accordingly, every node $C \in \mathbb{E}_{S,R,T_{S,R}}$ is regarded as interfering with and thus shall not transmit concurrently with the transmission from S to R.

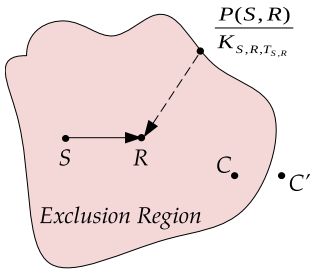

Fig. 1. PRK interference model

For enabling predictable interference control in the presence of network and environmental uncertainties, the parameter $K_{S,R,T_{S,R}}$ of the PRK model adapts to the specific network and environmental conditions to ensure the application-specific link reliability requirements. By ensuring the required link reliability and by using signal strength instead of geographic distance in model formulation, the PRK model captures the properties of wireless communication (e.g., cumulative interference, anisotropic signal propagation, and background noise) and thus is *of high-fidelity*. For enabling distributed protocol design and implementation, the PRK model is also *local*: 1) The parameters of the PRK model are either locally measurable (i.e., for the signal strength and link reliability between close-by nodes) or locally controllable (i.e., for $K_{S,R,T_{S,R}}$ of each link (S, R)), thus PRK-based scheduling does not need to rely on parameters such as nodes' locations or channel path loss between far-away nodes which are often used in physical-model-based scheduling [15] but are difficult to obtain precisely, especially in a distributed manner; 2) Only pairwise interference relations between close-by nodes need to be defined in the PRK model, thus PRK-based scheduling does not require explicit global coordination which is often used in physical-model-based scheduling [16], [17]. Through theoretical analysis based on stochastic geometry [6], simulation with 75,600 different network and environment settings,

and measurement in high-fidelity wireless network testbeds, Zhang et al. [6] have found that PRK-based scheduling can enable a channel spatial reuse very close to (e.g., $>95\%$) what is feasible in physical-model-based scheduling while ensuring application-required reliability.

Focusing on formulating the PRK interference model and understanding the theoretically achievable performance of PRK-based scheduling, Zhang et al. [6] left the design of distributed protocols for PRK-based scheduling as an open problem. Yet realizing distributed PRK-based scheduling in real-world settings poses the following *major challenges*:

- The parameter $K_{S,R,T_{S,R}}$ of the PRK model depends on the specific link (S, R), the application requirement on the link reliability (i.e., $T_{S,R}$), as well as the network and environmental conditions such as traffic pattern and wireless path loss which may well be dynamic and unpredictable, thus it is critical to instantiate the PRK model parameter $K_{S,R,T_{S,R}}$ on the fly depending on in-situ application requirements as well as network and environmental conditions; yet the relations between parameter $K_{S,R,T_{S,R}}$ and application requirements as well as network and environmental conditions are complex and difficult to characterize in closed-forms, which makes PRK model instantiation challenging.
- Given a link (S, R) and a specific instantiation of the PRK model, every node in the exclusion region $\mathbb{E}_{S,R,T_{S,R}}$ should be prevented from transmitting concurrently with the transmission from S to R. As we will discuss in detail in Sections III-C and III-D, however, it is difficult to ensure this property due to large interference range, anisotropy and asymmetry in wireless communication, as well as the delay in protocol signaling.

Contributions of this paper. To enable predictable link reliability in WNC systems, we address the aforementioned challenges by designing the distributed PRK-based scheduling protocol *PRKS*. In PRKS, we formulate the problem of identifying the PRK model parameter $K_{S,R,T_{S,R}}$ as a minimum-variance regulation control problem, and we design distributed controllers that allow each link to adapt its PRK model parameter for ensuring the desired link reliability through purely local coordination. For ensuring that nodes interfering with one another do not transmit concurrently, we propose the concept of local signal map that allows close-by nodes to maintain the wireless path loss among themselves; together with the PRK model, local signal maps enable nodes to precisely identify the interference relations among themselves despite large interference range and anisotropic, asymmetric wireless communication. To address the inherent delay in protocol signaling and to avoid interference between protocol signaling and data transmissions,

PRKS decouples protocol signaling from data transmission by leveraging the different timescales of PRK model adaptation and data transmission.

We have implemented PRKS in TinyOS. Through measurement study in the NetEye [18] and Indriya [19] wireless network testbeds, we demonstrate the following: 1) The distributed controllers enable network-wide convergence to a state where the desired link reliabilities are ensured; 2) With local, distributed coordination alone, PRKS achieves a channel spatial reuse very close to what is enabled by the state-of-the-art centralized physical-model-based scheduler iOrder [20] while ensuring the required link reliability; 3) Unlike existing scheduling protocols where link reliability is unpredictable and the ratio of links whose reliability meets application requirements can be as low as 0%, PRKS enables predictably high link reliability (e.g., 95%) for all the links in different network and environmental conditions without a priori knowledge of these conditions; 4) By ensuring the required link reliability in scheduling, PRKS also enables a lower communication delay and a higher network throughput than existing scheduling protocols.

Organization of the paper. We present in Section II the network and traffic models as well as the wireless network testbeds used in this study. Then we elaborate on the design of PRKS in Section III, and we evaluate the performance of PRKS in Section IV. We discuss related work in Section V, and we make concluding remarks in Section VI.

II. Preliminaries

Network and traffic models & problem definition. As a first-step towards ensuring predictable link reliability in distributed scheduling, we consider mostly-immobile wireless control networks where nodes are statically deployed and are fixed at specific locations most of the time even though they may be moved around infrequently. In such networks, the average background noise power and the average wireless path loss tend to be stable at timescales of seconds, minutes, or even longer [21]. Focusing on predictable co-channel interference control, we also only consider the cases when the data transmission power along a link is fixed even though different links may use different transmission powers; mobile networks and data transmission power control are relegated as future research.

Focusing on interference-oriented scheduling of data transmissions at the link layer, our study considers one-hop data transmissions between close-by nodes, but the network itself is multi-hop and with nodes widely distributed in space. Note that predictable reliability in one-hop transmissions is important by itself for new networked control paradigms that involve

communications between close-by nodes only [14], and predictably reliable one-hop transmission is also a basis for reliable multi-hop transmission in general as we show in [12].

With the above network and traffic settings, we study the online slot-scheduling problem [20] where, given a set of links in a multi-hop network at any time instant, a maximal subset of the links need to be scheduled in a distributed manner to transmit concurrently while ensuring that the mean packet delivery reliability (PDR) across each of the scheduled links is no less than an application-required PDR across the link. To leverage the locality and high-fidelity of the PRK model, we investigate PRK-based online slot-scheduling.

Wireless network testbeds. The measurement parts of our study use a publicly available wireless network testbed NetEye [18]. In a large lab space, NetEye deploys 130 TelosB motes in a grid with every two closest neighboring motes separated by 2 feet (i.e., 0.61 meter). The grid deployment enables the study of both grid networks and random networks, where random networks can be generated using a subset of the 130 motes in experiments (e.g., using each mote with a certain probability). Zhang et al. [6] have shown that, despite its seemingly uniform deployment pattern, NetEye embodies many of the complexities and heterogeneity experienced in outdoor, real-world deployments; for instance, there is a high degree of variability in the background noise power at nodes and in the packet delivery reliabilities for links of equal length, thus reflecting non-uniform network settings as seen in practice. Each of these TelosB motes is equipped with a 3dB signal attenuator and a 2.45GHz monopole antenna. Unless mentioned otherwise, we use a radio transmission power of -25dBm (i.e., power level 3 in TinyOS) for data packets such that the data transmission reliability is over 95% in the absence of interference for links up to 6 feet (i.e., 1.83 meters) long.

Considering the high fidelity of NetEye, we mainly present our measurement results in NetEye, but we verify key observations using the Indriya testbed [19]. Indriya deploys 139 TelosB motes across three floors of the School of Computing at the National University of Singapore; its sparse node distribution in a 3D space represents a network and environmental setting different from that of NetEye.

III. PRK-BASED SCHEDULING

A. Overview

Here we present an overview of our approaches to addressing the challenges of PRK-based scheduling as discussed in Section I. To instantiate the PRK model parameter according to in-

situ network and environmental condition as well as application requirement on link reliability, we model the PRK model instantiation problem as a *regulation control* problem [22], and we leverage communication theory and model predictive control theory to derive the optimal controller that ensures application-required link reliability. Each link executes the controller in a distributed manner to instantiate and adapt its PRK model parameter according to in-situ network and environmental condition as well as application requirement on link reliability. To apply the instantiated PRK model in identifying mutual interference relations between links, we observe that the PRK model is defined based on wireless signal power between nodes and the instantiated PRK model parameter. Accordingly, we propose to have close-by nodes maintain *local signal maps* that identify wireless signal power attenuation between themselves, which can be accomplished through received-signal-strength-indicator (RSSI) sampling at each node. Using the signal maps, instantiated PRK model parameters, and knowledge of nodes' transmission powers, each node can identify in a distributed manner the set of other links whose transmissions interfere with its own transmission. Based on mutual interference relations between links, data transmissions along different links can be scheduled in a TDMA manner to ensure predictable interference control and thus predictable link reliability.

To integrate the above approaches into a field-deployable solution, we propose the distributed PRK-based scheduling protocol *PRKS* whose architecture is shown in Figure 2. In PRKS, data packet transmissions are executed in the data plane, and their transmission status (i.e., success or failure) serve as the feedback to the control plane which schedules data transmissions to ensure application-required link reliability. In particular, the status of data transmissions are used by individual links to estimate their in-situ link reliabilities, which in turn triggers the PRK model adaptations at individual links. The instantiated PRK model parameters are used together with signal maps to identify interference relations between transmissions, which in turn are used to enable TDMA

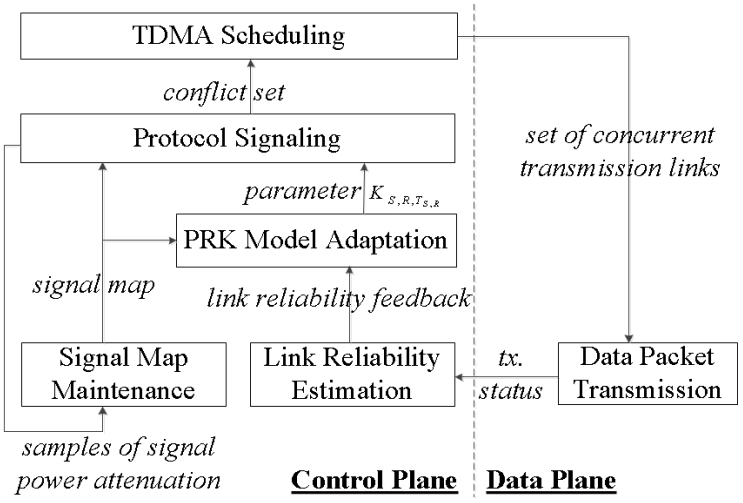

Fig. 2. Architecture of PRKS

scheduling with predictable link reliability.

In what follows, we elaborate on the individual components of the PRKS scheduling protocol. We first present our control-theoretic approach to instantiating the PRK model in Section III-B, then we present our protocol signaling method based on local signal maps in Section III-C, and we present the detailed design and operation of the PRKS protocol in Section III-D.

B. A control-theoretic approach to PRK model instantiation

Model predictive regulation control. Given a link (S, R), the task of instantiating the PRK interference model is to identify the parameter $K_{S,R,T_{S,R}}$ such that the resulting scheduling can ensure the required minimum link reliability $T_{S,R}$.[1] It is, however, difficult to characterize the relation between $K_{S,R,T_{S,R}}$ and the packet delivery reliability along (S, R) in closed-form, and the relation is complex and dependent on network and environmental conditions which may well be unpredictable at design time [6]. To address the challenge, we observe that the PRK model instantiation problem can be formulated as an online *regulation control* problem [22], where the "plant" is the link (S, R), the "reference input" is the required link reliability $T_{S,R}$, the "plant output" is the actual link reliability $Y_{S,R}$ from S to R, the "control input" is the PRK model parameter $K_{S,R,T_{S,R}}$, and the objective of the regulation control is to adjust the control input so that the plant output is as close to the reference input as possible. To address the difficulty in characterizing the "plant model" on the relation between the control input $K_{S,R,T_{S,R}}$ and the plant output $Y_{S,R}$, we observe that changing the PRK model parameter $K_{S,R,T_{S,R}}$ changes the exclusion region around the receiver R and thus the concurrent transmissions along with the transmission from S to R, which in turn leads to the change in the average interference power at receiver R. Accordingly, we propose to regard this change in interference power, denoted by ΔI_R, as the actual control input. This way, we can leverage the existing communication theory to derive the plant model on the relation between $Y_{S,R}$ and ΔI_R as follows.

For conciseness, we use $\tilde{I}_R(t)$ and $I_R(t)$ to denote, in units of dBm, the sum of the background noise power and the power of all interfering signals at the receiver R and its average respectively at time instant t ($t = 1, 2, \ldots$), with $\tilde{I}_R(t) = I_R(t) + \xi_R(t)$ and $\xi_R(t)$ being a zero-mean random variable. Assuming a discrete-time model where the changes in the average background noise power and average wireless channel path loss from a time instant t to the next time instant $t+1$

[1]Focusing on interference-oriented scheduling, we only consider the links whose packet delivery reliabilities are above the required ones in the absence of interference.

are negligible as compared with the background noise power and wireless channel path loss themselves, $I_R(t+1)$ may differ from $I_R(t)$ for two possible reasons:[2]

- From time instant t to $t+1$, the PRK model parameter may change from $K_{S,R,T_{S,R}}(t)$ to $K_{S,R,T_{S,R}}(t+1)$. Accordingly, the exclusion region around the receiver R changes from $\mathbb{E}_{S,R,T_{S,R}}(t)$ to $\mathbb{E}_{S,R,T_{S,R}}(t+1)$. If $K_{S,R,T_{S,R}}(t+1) > K_{S,R,T_{S,R}}(t)$, nodes in $\mathbb{E}_{S,R,T_{S,R}}(t+1) \setminus \mathbb{E}_{S,R,T_{S,R}}(t)$ may transmit concurrently with the transmission from S to R and thus introduce interference to R at time t but not at time $t+1$; similarly, if $K_{S,R,T_{S,R}}(t+1) < K_{S,R,T_{S,R}}(t)$, nodes in $\mathbb{E}_{S,R,T_{S,R}}(t) \setminus \mathbb{E}_{S,R,T_{S,R}}(t+1)$ may introduce interference to R at time $t+1$ but not at time t. We use $\Delta I_R(t)$ to denote the average interference change at receiver R due to the change of the PRK model parameter from t to $t+1$. Since the receiver R can control the changes of the PRK model parameter as we will discuss shortly, $\Delta I_R(t)$ can be controlled by the receiver R and is thus treated as the "control input".
- The set of nodes that are not in the exclusion region around the receiver R at time instants t and $t+1$ and are scheduled to transmit concurrently with the link (S,R) may change from time t to $t+1$. Accordingly, the average interference introduced by nodes outside the exclusion region around R changes from t to $t+1$, and we use $\Delta I_U(t)$ to denote this change. Since $\Delta I_U(t)$ is beyond the local control of link (S,R), we treat $\Delta I_U(t)$ as a "disturbance" to the system and denote the mean of $\Delta I_U(t)$ as $\mu_U(t)$. $\Delta I_U(t)$ tends to be uncorrelated with $\Delta I_R(t)$.

Therefore,

$$I_R(t+1) = I_R(t) + \Delta I_R(t) + \Delta I_U(t), \quad \tilde{I}_R(t+1) = I_R(t+1) + \xi_R(t+1),$$

where $\Delta I_R(t)$ and $\Delta I_U(t)$ are in units of dB, and $\xi_R(t+1)$ is a zero-mean random variable reflecting the impact of factors such as small-scale channel fading.

We use $\tilde{P}_{S,R}(t)$ and $P_{S,R}(t)$ to denote the received data signal power from S to R (in units of dBm) and its average at time instant t respectively, then communication theory and practice imply the following [6], [23]:

$$Y_{S,R}(t) = f_0(\tilde{P}_{S,R}(t) - \tilde{I}_R(t), t) = f_1(P_{S,R}(t) - I_R(t)) + \xi_f(t), \tag{1}$$

[2]In protocol implementation, the actual time interval between t and $t+1$ can be chosen to be the small interval required for computing a sample of link reliability.

where $P_{S,R}(t) - I_R(t)$ approximates, in units of dBs, the signal-to-interference-plus-noise-ratio (SINR) at time instant t, $f_1(.)$ is a non-linear, increasing function of $P_{S,R}(t) - I_R(t)$ with the specific function form dependent on the modulation and coding schemes used by the radio, and $\xi_f(t)$ is a small, bounded, and zero-mean random perturbation depending on the in-situ network and environmental conditions [23]. Therefore, the "plant model" for link (S, R) is

$$\begin{aligned} \tilde{I}_R(t+1) &= I_R(t+1) + \xi_R(t+1) = I_R(t) + \Delta I_R(t) + \Delta I_U(t) + \xi_R(t+1) \\ \tilde{P}_{S,R}(t+1) &= P_{S,R}(t+1) + \xi_P(t+1) = P_{S,R}(t) + \xi_P(t+1) \\ Y_{S,R}(t+1) &= f_0(\tilde{P}_{S,R}(t+1) - \tilde{I}_R(t+1), t+1) \end{aligned} \tag{2}$$

where $(\tilde{I}_R(.), \tilde{P}_{S,R}(.))$ and $Y_{S,R}(.)$ are the "state" and the "output" of the plant respectively, and the objective of the control problem at time t is to select the control input $\Delta I_R(t)$ such that $Y_{S,R}(t+1)$ is as close to the required link reliability $T_{S,R}$ as possible.

To address the challenges of the nonlinearity and time-dependence of function $f_0(.)$ in control design, we observe that, for the control problem mentioned above, we only needs to find another function $f(.)$ that approximates well $f_0(.)$ at the current system operating point $(\tilde{P}_{S,R}(t) - \tilde{I}_R(t), Y_{S,R}(t))$ and the target equilibrium point $(f_1^{-1}(T_{S,R}), T_{S,R})$ where the required communication reliability is satisfied. To this end, we approximate function $f_0(.)$, at time t, by the following affine function $f(.)$ in the neighborhood of the target equilibrium point $(f_1^{-1}(T_{S,R}), T_{S,R})$:

$$\begin{aligned} &f(x) = a(t)x + b(t), \\ &\text{where } a(t) = g(Y_{S,R}(t), P_{S,R}(t), I_R(t), T_{S,R}) = \tfrac{T_{S,R} - Y_{S,R}(t)}{f_1^{-1}(T_{S,R}) - (P_{S,R}(t) - I_R(t))}, \\ &\qquad b(t) = T_{S,R} - a(t) f_1^{-1}(T_{S,R}). \end{aligned} \tag{3}$$

As shown in Figure 3, function $f(.)$ cuts across the current system operating point $(P_{S,R}(t) - I_R(t), Y_{S,R}(t))$ and the target equilibrium point $(f_1^{-1}(T_{S,R}), T_{S,R})$. Therefore, we use the following approximate plant model at time t:

$$\begin{aligned} I_R(t+1) &= I_R(t) + \Delta I_R(t) + \Delta I_U(t) \\ P_{S,R}(t+1) &= P_{S,R}(t) \\ Y_{S,R}(t+1) &= a(t)(P_{S,R}(t+1) - I_R(t+1)) + b(t) \end{aligned} \tag{4}$$

Accordingly, the system model is as shown in Figure 4, where $\overline{Y}_{S,R}(t) = c\overline{Y}_{S,R}(t-1) + (1-c)Y_{S,R}(t)$, $0 \leq c < 1$, with $\overline{Y}_{S,R}(1)$ initialized as $Y_{S,R}(1)$. To smooth out the time-varying randomness in $Y_{S,R}(.)$, the exponentially-weighted-moving-average (EWMA) filter in the feedback loop is introduced to track the link reliability $Y_{S,R}(.)$ such that $E[\overline{Y}_{S,R}(t)] = E[Y_{S,R}(t)]$

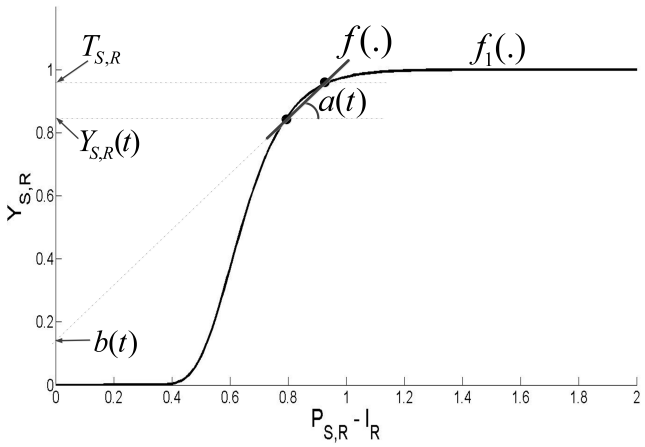

Fig. 3. Affine approximation of function $f_0(.)$ by $f(.)$ in the neighborhood of the expected equilibrium point $(f_1^{-1}(T_{S,R}), T_{S,R})$ at time t

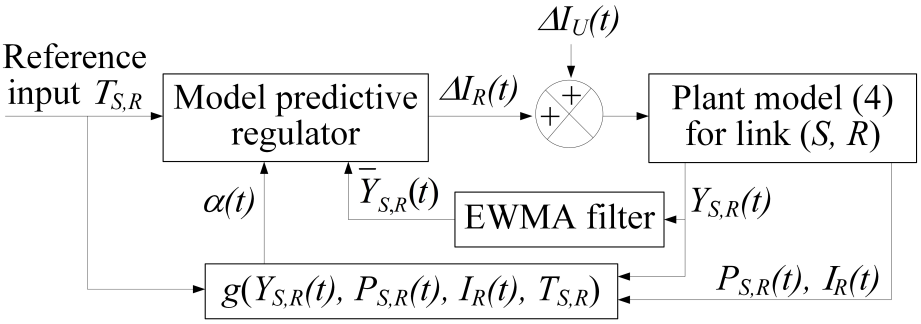

Fig. 4. System diagram of PRK model instantiation as model predictive regulation control

but $\overline{Y}_{S,R}(t)$ has smaller variability than $Y_{S,R}(t)$. The weight factor c determines the tradeoff between the stability and agility of the EWMA filter; the larger the c is, the more stable the filter. In our implementation, we have tried different values of c, and we find setting c as a relatively large value (e.g., $\frac{15}{16}$) is a good choice in enabling stable link reliability.

Given the probabilistic nature of wireless communication, the link reliability $\overline{Y}_{S,R}(t)$ is expected to be inherently random. To control $\overline{Y}_{S,R}(t)$ to be as close to the desired reliability $T_{S,R}$ as possible, we need to minimize $E[(\overline{Y}_{S,R}(t) - T_{S,R})^2]$. More formally, the control design at time t is a model predictive control problem as follows:

$$\begin{aligned} \min_{\Delta I_R(t)} \quad & E[(\overline{Y}_{S,R}(t+1) - T_{S,R})^2] \\ \text{subject to} \quad & \overline{Y}_{S,R}(t+1) = c\overline{Y}_{S,R}(t) + (1-c)Y_{S,R}(t+1), \\ & \text{Plant model (4) for link } (S,R). \end{aligned} \tag{5}$$

For this control problem, we have

Theorem 1: The optimal solution to Problem (5) is

$$\Delta I_R(t) = \frac{(1+c)\overline{Y}_{S,R}(t) - c\overline{Y}_{S,R}(t-1) - T_{S,R}}{(1-c)a(t)} - \mu_U(t). \tag{6}$$

Applying the above optimal control input $\Delta I_R(t)$ at time t makes $E[\overline{Y}_{S,R}(t+1)] = T_{S,R}$ and the variance of $\overline{Y}_{S,R}(t+1)$ minimum.

Proof:

$$\begin{aligned}
E[(\overline{Y}_{S,R}(t+1) - T_{S,R})^2] &= E[(c\overline{Y}_{S,R}(t) + (1-c)Y_{S,R}(t+1) - T_{S,R})^2] \\
&= E[(c\overline{Y}_{S,R}(t) + (1-c)(a(t)(P_{S,R}(t+1) - I_R(t+1)) + b(t)) - T_{S,R})^2] \\
&= E[(c\overline{Y}_{S,R}(t) + (1-c)(a(t)(P_{S,R}(t+1) - I_R(t+1)) + b(t)) - T_{S,R} - \\
&\quad (1-c)a(t)(\mu_U(t) - \mu_U(t)))^2] \\
&= E[(X - (1-c)a(t)(\Delta I_U(t) - \mu_U(t)))^2],
\end{aligned}$$

where $X = c\overline{Y}_{S,R}(t) + (1-c)(a(t)(P_{S,R}(t+1) - I_R(t)) + b(t)) - T_{S,R} - (1-c)a(t)\mu_U(t) - (1-c)a(t)\Delta I_R(t)$.

At time t, $a(t)$ is given and $E[\Delta I_U(t) - \mu_U(t)] = 0$. Thus $E[(1-c)a(t)(\Delta I_U(t) - \mu_U(t))] = (1-c)a(t)E[\Delta I_U(t) - \mu_U(t)] = 0$. Given that X and $\Delta I_U(t)$ are uncorrelated, we need $X = 0$ to minimize $E[(\overline{Y}_{S,R}(t) - T_{S,R})^2]$. Accordingly, the control input that minimizes $E[(\overline{Y}_{S,R}(t) - T_{S,R})^2]$ at time t is as follows:

$$\Delta I_R(t) = \frac{c\overline{Y}_{S,R}(t) + (1-c)[a(t)[P_{S,R}(t+1) - I_R(t)] + b(t)] - T_{S,R}}{(1-c)a(t)} - \mu_U(t).$$

Since $P_{S,R}(t+1) = P_{S,R}(t)$, we have

$$\begin{aligned}
\Delta I_R(t) &= \frac{c\overline{Y}_{S,R}(t) + (1-c)[a(t)[P_{S,R}(t) - I_R(t)] + b(t)] - T_{S,R}}{(1-c)a(t)} - \mu_U(t) \\
&= \frac{c\overline{Y}_{S,R}(t) + (1-c)Y_{S,R}(t) - T_{S,R}}{(1-c)a(t)} - \mu_U(t) \\
&= \frac{c\overline{Y}_{S,R}(t) + \overline{Y}_{S,R}(t) - c\overline{Y}_{S,R}(t-1) - T_{S,R}}{(1-c)a(t)} - \mu_U(t) \\
&= \frac{(1+c)\overline{Y}_{S,R}(t) - c\overline{Y}_{S,R}(t-1) - T_{S,R}}{(1-c)a(t)} - \mu_U(t).
\end{aligned}$$

Given the above control input $\Delta I_R(t)$ and considering that $P_{S,R}(t+1) = P_{S,R}(t)$, we have

$$\begin{aligned}
\overline{Y}_{S,R}(t+1) &= c\overline{Y}_{S,R}(t) + (1-c)[a(t)(P_{S,R}(t+1) - I_R(t+1)) + b(t)] \\
&= c\overline{Y}_{S,R}(t) + (1-c)[a(t)(P_{S,R}(t+1) - I_R(t) - \Delta I_R(t) - \Delta I_U(t)) + b(t)] \\
&= c\overline{Y}_{S,R}(t) + (1-c)[a(t)(P_{S,R}(t+1) - I_R(t) - \frac{c\overline{Y}_{S,R}(t) + (1-c)Y_{S,R}(t) - T_{S,R}}{(1-c)a(t)} + \mu_U(t) - \Delta I_U(t)) + b(t)] \\
&= c\overline{Y}_{S,R}(t) + (1-c)[a(t)(P_{S,R}(t+1) - I_R(t) - \frac{c\overline{Y}_{S,R}(t) + (1-c)[a(t)[P_{S,R}(t+1) - I_R(t)] + b(t)] - T_{S,R}}{(1-c)a(t)} + \\
&\quad \mu_U(t) - \Delta I_U(t)) + b(t)] \\
&= T_{S,R} + (1-c)a(t)(\mu_U(t) - \Delta I_U(t)).
\end{aligned}$$

Since $E[(1-c)a(t)(\mu_U(t)-\Delta I_U(t))]=0$, $E[\overline{Y}_{S,R}(t+1)]=T_{S,R}$ indeed holds. With $E[\overline{Y}_{S,R}(t+1)]=T_{S,R}$, the objective function (5) is the variance of $\overline{Y}_{S,R}(t+1)$]. Hence applying the optimal control input $\Delta I_R(t)$ at time t also minimizes the variance of $\overline{Y}_{S,R}(t+1)$. ■

From $\Delta I_R(t)$ to $K_{S,R,T_{S,R}}(t+1)$. Given that it is convenient for the receiver R to measure link reliability $\overline{Y}_{S,R}(t)$ [8], we propose to execute the model predictive regulation controller (6) at R. Using similar techniques as what we will discuss in Section III-C, R can also measure $P_{S,R}(t)$ and $I_R(t)$, thus R can compute $a(t)$. For each time instant t, R can also derive $\Delta I_U(t-1)$ based on $I_R(t)$, $I_R(t-1)$, $\Delta I_R(t-1)$, and Equation (2); using these derived samples of $I_U(.)$ and an EWMA filter, R can then estimate $\mu_U(.)$. Therefore, R can execute the controller (6) using information that is either locally measured (e.g., for $\overline{Y}_{S,R}(t)$ and $\overline{Y}_{S,R}(t-1)$) or locally derived (e.g., for $a(t)$ and $\mu_U(t)$).

After R computes the control input $\Delta I_R(t)$ at time t, R needs to compute $K_{S,R,T_{S,R}}(t+1)$ so that

$$\begin{cases} K_{S,R,T_{S,R}}(t+1)=K_{S,R,T_{S,R}}(t), & \text{if } \Delta I_R(t)=0 \\ K_{S,R,T_{S,R}}(t+1)>K_{S,R,T_{S,R}}(t), & \text{if } \Delta I_R(t)<0 \\ K_{S,R,T_{S,R}}(t+1)<K_{S,R,T_{S,R}}(t), & \text{if } \Delta I_R(t)>0 \end{cases} \tag{7}$$

and that, when the PRK model parameter is $\min\{K_{S,R,T_{S,R}}(t), K_{S,R,T_{S,R}}(t+1)\}$, the expected interference introduced to R by the nodes in either $\mathbb{E}_{S,R,T_{S,R}}(t)$ or $\mathbb{E}_{S,R,T_{S,R}}(t+1)$ but not in both is as close to $|\Delta I_R(t)|$ as possible while ensuring that the expected link reliability is no less than $T_{S,R}$ when the PRK model parameter is $K_{S,R,T_{S,R}}(t+1)$.[3] To realize this, we define, for each node C that may be included in the exclusion region of R during network operation, the expected interference $I(C,R,t)$ that C introduces to R when C is not in the exclusion region of R. Then $I(C,R,t)=\beta_C(t)P(C,R,t)$, where $\beta_C(t)$ is the probability for C to transmit data packets at time t and $P(C,R,t)$ is the power strength of the data signals reaching R from C.[4] Considering the discrete nature of node distribution in space and the requirement on satisfying the minimum link reliability $T_{S,R}$, we propose the following rule for computing $K_{S,R,T_{S,R}}(t+1)$:

- When $\Delta I_R(t)=0$, let $K_{S,R,T_{S,R}}(t+1)=K_{S,R,T_{S,R}}(t)$.

[3]Due to the discrete nature of node distribution, the resulting link reliability may be slightly higher than the required reliability $T_{S,R}$ instead of being exactly equal to $T_{S,R}$.

[4]$P(C,R,t)$ and $\beta_C(t)$ can be estimated through purely local coordination between R and C using the protocol signaling mechanism of Section III-C.

- When $\Delta I_R(t) < 0$ (i.e., need to expand the exclusion region), let $\mathbb{E}_{S,R,T_{S,R}}(t+1) = \mathbb{E}_{S,R,T_{S,R}}(t)$, then keep adding nodes not already in $\mathbb{E}_{S,R,T_{S,R}}(t+1)$, in the non-increasing order of their data signal power at R, into $\mathbb{E}_{S,R,T_{S,R}}(t+1)$ until the node B such that adding B into $\mathbb{E}_{S,R,T_{S,R}}(t+1)$ makes $\sum_{C\in\mathbb{E}_{S,R,T_{S,R}}(t+1)\setminus\mathbb{E}_{S,R,T_{S,R}}(t)} I(C,R,t) \geq |\Delta I_R(t)|$ for the first time. Then let $K_{S,R,T_{S,R}}(t+1) = \frac{P(S,R,t)}{P(B,R,t)}$.
- When $\Delta I_R(t) > 0$ (i.e., need to shrink the exclusion region), let $\mathbb{E}_{S,R,T_{S,R}}(t+1) = \mathbb{E}_{S,R,T_{S,R}}(t)$, then keep removing nodes out of $\mathbb{E}_{S,R,T_{S,R}}(t+1)$, in the non-decreasing order of their data signal power at R, until the node B such that removing any more node after removing B makes $\sum_{C\in\mathbb{E}_{S,R,T_{S,R}}(t)\setminus\mathbb{E}_{S,R,T_{S,R}}(t+1)} I(C,R,t) > |\Delta I_R(t)|$ for the first time. Then let $K_{S,R,T_{S,R}}(t+1) = \frac{P(S,R,t)}{P(B,R,t)}$.

For convenience, we call the above rule the *PRK-model-adaptation* rule. In our study, we set the initial value of the PRK model parameter such that the initial exclusion region around R includes every strong interferer whose transmission alone, concurrent with the transmission from S to R, can make the link reliability drop below $T_{S,R}$. This way, the initial link reliability is not too far away from $T_{S,R}$, which helps ensure the goodness of approximating function $f_0(.)$ by $f(.)$ in the neighborhood of the desired link reliability $T_{S,R}$.

With the model predictive regulation controller (6) and the PRK-model-adaptation rule discussed above, scheduling based on the instantiated PRK model ensures the required link reliability. Formally, we have

Theorem 2: Applying the PRK-model-adaptation rule and the control input $\Delta I_R(t+i) = \frac{(1+c)\overline{Y}_{S,R}(t+i)-c\overline{Y}_{S,R}(t+i-1)-T_{S,R}}{(1-c)a(t+i)} - \mu_U(t+i)$ $(i=0,1,\ldots)$ starting at a time instant t, $E[\overline{Y}_{S,R}(t+1+i)] \geq T_{S,R}$ $(i=0,1,\ldots)$.

Proof: Let $\Delta\hat{I}_R(t) = \sum_{C\in(\mathbb{E}_{S,R,T_{S,R}}(t+1)\setminus\mathbb{E}_{S,R,T_{S,R}}(t))\cup(\mathbb{E}_{S,R,T_{S,R}}(t)\setminus\mathbb{E}_{S,R,T_{S,R}}(t+))} I(C,R,t))$, i.e., the absolute value of the change of the average interference power at the receiver R due to the change of the PRK model parameter from t to $t+1$. Applying the PRK-model-adaptation rule and the predictive minimum-variance regulation control (5) at a time instant t, $E[\overline{Y}_{S,R}(t+1)] = T_{S,R}$ if $\Delta\hat{I}_R(t) = |\Delta I_R(t)|$. Due to the discrete nature of node distribution, however, it may well be the case that $\Delta\hat{I}_R(t) \neq |\Delta I_R(t)|$. In this case, if $\Delta I_R(t) < 0$, applying the PRK-model-adaptation rule will expand the exclusion region such that $\Delta\hat{I}_R(t) > |\Delta I_R(t)|$, which makes $E[\overline{Y}_{S,R}(t+1)] > T_{S,R}$; on the other hand, if $\Delta I_R(t) > 0$, applying the PRK-model-adaptation rule will shrink the exclusion region such that $\Delta\hat{I}_R(t) < |\Delta I_R(t)|$, which also makes $E[\overline{Y}_{S,R}(t+1)] > T_{S,R}$. Therefore, $E[\overline{Y}_{S,R}(t+1)] > T_{S,R}$ holds if $\Delta\hat{I}_R(t) \neq |\Delta I_R(t)|$. For the

same reasons as above, $E[\overline{Y}_{S,R}(t+2+i)] \geq T_{S,R}$ $(i = 0, 1, \ldots)$ holds. ■

From Theorem 2, it takes one control step (i.e., one adaptation of the PRK model parameter) for the PRK model parameter to converge to a state where the required link reliability is satisfied. In practice, due to the use of the approximate function $f(.)$ and the imperfection in estimating parameters such as $\mu_U(t)$ and $\beta_C(t)$ (which are used in the $\Delta I_R(t)$ calculation and in the PRK-model-adaption rule respectively), it takes more than one control step for the PRK model parameter to converge. As we will present in our testbed-based measurement study in Section IV, however, the PRK model parameters of all the links still converge quickly to a state where the required link reliabilities are satisfied, for instance, with a median convergence time of 22 control steps.

C. Protocol signaling for real-world use of the PRK model

Given a link (S, R) and a specific instantiation of the PRK model, the parameter $K_{S,R,T_{S,R}}(t)$ defines an exclusion region $\mathbb{E}_{S,R,T_{S,R}}(t)$ around the receiver R such that a node $C \in \mathbb{E}_{S,R,T_{S,R}}(t)$ if and only if $P(C, R, t) \geq \frac{P(S,R,t)}{K_{S,R,T_{S,R}}(t)}$. In PRK-based scheduling, every node $C \in \mathbb{E}_{S,R,T_{S,R}}(t)$ should be aware of its existence in $\mathbb{E}_{S,R,T_{S,R}}(t)$ and should not transmit concurrently with the reception at R. Yet it is challenging to ensure this property for the following real-world complexities in wireless communication: 1) node C may be located beyond the communication range of R such that it is challenging for R to inform C of its state (e.g., the value of $K_{S,R,T_{S,R}}(t)$); 2) wireless communication may be anisotropic such that it is difficult for R to transmit protocol signaling messages that reach and only reach nodes in $\mathbb{E}_{S,R,T_{S,R}}(t)$; 3) wireless communication may be asymmetric such that nodes interfering with one another may not know one another's state (e.g., $K_{S,R,T_{S,R}}(t)$).

Local signal maps. To address these challenges, we propose that every node R maintains a *local signal map* that contains the average signal power attenuation between R and every node C close-by.[5] To identify the signal power attenuation $P'(C, R)$ from a node C to another node R, C can inform R of the transmission power P_C used for a data or control packet that C transmits to R by piggybacking P_C onto the packet, and then R can derive the power attenuation as long as R can estimate the power of the received signals from C, denoted by $P(C, R)$. To this end, R samples the RSSI value P_{total} at an instant right before finishing

[5]The exact set of close-by nodes that shall be included in the signal map will be discussed shortly.

receiving a packet from C, and, immediately after receiving the packet, R samples the RSSI value P_I again. As shown in Figure 5, P_I is the sum of the background noise power and the interference power at R right after the packet reception, and $P_{total} = P(C,R) + P'_I$ where P'_I is the sum of the background noise power and the interference power at R right before the packet reception. As we will discuss in Section III-D, signal maps are maintained in the control plane of the protocol PRKS where wireless channel access is based on the traditional random access method CSMA/CA as used in IEEE 802.15.4 and 802.11. Given that P_{total} and P_I can be sampled at very short interval (e.g., less than 0.01 milliseconds for TelosB motes [24]) and that the background noise power as well as the interference power do not change much in such short intervals in CSMA/CA-based wireless networks, the sum of the background noise power and the interference power do not change much immediately before and immediately after a packet reception, i.e., $P'_I \approx P_I$. Thus,

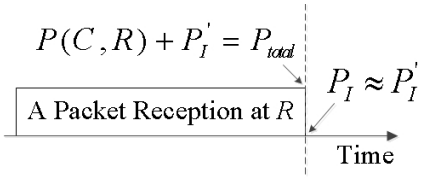

Fig. 5. Estimation of signal power attenuation

$$P(C,R) = P_{total} - P'_I \approx P_{total} - P_I. \tag{8}$$

Once R gets a sample of $P(C,R)$, it can compute a sample of $P'(C,R)$ as $P_C - P(C,R)$. This way, R can get a series of samples of $P'(C,R)$ and then use these samples to derive the average signal power loss from C to itself.

Using the above method of sampling signal power attenuation, nodes close-by can establish their local signal maps through purely local sampling of their packet receptions without any global coordination in the network, and the local signal maps generated in this manner tend to be very accurate too. For instance, Figure 6 shows the CDF of the relative errors[6] in estimating power attenuation across links in the NetEye [18] sensor network testbed when all the 130 TelosB motes transmit packets using the CSMA/CA-based B-MAC [25] and at an average inter-packet interval of 25 seconds, 2.5 seconds, and 0.1 seconds respectively, which we denote as light traffic, medium traffic, and heavy traffic respectively.

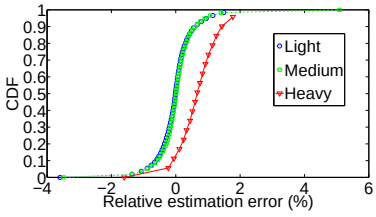

Fig. 6. Relative errors in estimating link signal power attenuation in NetEye

[6]The relative error for a link is defined as the estimated attenuation minus the ground-truth attenuation and then divided by the ground-truth attenuation.

We see that the estimation is quite accurate. For instance, the relative estimation errors are all very close to 0 and almost always within $[-2\%, 2\%]$; in addition, the 95% confidence interval for the median relative error is $[-0.0508\%, 0.0535\%]$, $[-0.0152\%, 0.0280\%]$, and $[-0.0087\%, 0.0245\%]$ for the light, medium, and heavy traffic condition respectively, thus the median estimation error is 0 at the 95% confidence level for all traffic conditions. We have also observed similar accuracy for estimating link power attenuation in the Indriya testbed [19], showing the effectiveness of our method of signal power attenuation estimation in different network and traffic conditions; interested readers can find more detailed validation results for our estimation method in [12].

For protocol signaling in PRK-based scheduling, the local signal maps maintain bi-directional power attenuation between each pair of close-by nodes. After estimating $P'(C, R)$, for instance, R informs C of $P'(C, R)$ so that C is aware of the power attenuation from itself to R.

Protocol signaling based on signal maps. For ensuring awareness of mutual interference between nodes, the PRK model parameter $K_{S,R,T_{S,R}}(t)$ of each link (S, R) needs to be known by every node C in the exclusion region $\mathbb{E}_{S,R,T_{S,R}}(t)$. To this end, node R broadcasts signaling packets with the value of $K_{S,R,T_{S,R}}(t)$ piggybacked, so that nodes within the communication range of R get to know $K_{S,R,T_{S,R}}(t)$. To ensure that $K_{S,R,T_{S,R}}(t)$ is also known to every node C that is in $\mathbb{E}_{S,R,T_{S,R}}(t)$ but is beyond the communication range of R, every node C' that has learned $K_{S,R,T_{S,R}}(t)$ and is in $\mathbb{E}_{S,R,T_{S,R}}(t)$ can rebroadcast a signaling packet with the value of $K_{S,R,T_{S,R}}(t)$ piggybacked, which enables every node $C \in \mathbb{E}_{S,R,T_{S,R}}(t)$ to learn about $K_{S,R,T_{S,R}}(t)$. In this process, a node C' can check whether it is in $\mathbb{E}_{S,R,T_{S,R}}(t)$ by checking, based on its local signal map, whether $P(C', R, t) \geq \frac{P(S,R,t)}{K_{S,R,T_{S,R}}(t)}$. Therefore, local signal maps enable addressing the challenge of large interference range in inter-node coordination through signaling-packet relay/rebroadcast within exclusion regions. To reduce the number of rebroadcasts needed for all the nodes in $\mathbb{E}_{S,R,T_{S,R}}(t)$ to learn about $K_{S,R,T_{S,R}}(t)$, certain rebroadcasts are suppressed based on well-known broadcast-suppression techniques [26], for instance, giving nodes with lower interference power to R (i.e., "farther away" from R in the signal map) higher priority in rebroadcasting and suppressing a node's rebroadcast if it has heard rebroadcasts from several close-by nodes.

Once a node C learns about the value of $K_{S,R,T_{S,R}}(t)$, C can use its local signal map to decide whether its transmission may interfere with the transmission from S to R (i.e., whether $C \in \mathbb{E}_{S,R,T_{S,R}}(t)$) by checking whether $P(C, R, t) \geq \frac{P(S,R,t)}{K_{S,R,T_{S,R}}(t)}$. Therefore, signaling packets can reach nodes not in $\mathbb{E}_{S,R,T_{S,R}}(t)$ without falsely including those nodes into $\mathbb{E}_{S,R,T_{S,R}}(t)$, thus

addressing the challenge of anisotropic wireless communication. Using local signal maps and with signaling-packet relay as discussed above, a pair of nodes C and R can inform each other of their respective states (e.g., the PRK model parameter and the data transmission probability) even if communications between C and R are asymmetric, thus addressing the challenge of asymmetric wireless communication in protocol signaling.

For the correctness of the above protocol signaling method, the local signal map of a node R should include the set $\mathbb{E}'$ of nodes whose transmission may interfere with the reception at R or whose reception may be interfered by the transmission by R (e.g., the transmission of ACK packets by R). Since the set $\mathbb{E}'$ may well be dynamic and uncertain depending on network and environmental conditions, a node R dynamically adjusts the set of nodes in its local signal map through local coordination with nodes close-by, and R may also maintain a relatively large signal map to include the nodes that may be in $\mathbb{E}'$ over time.

Together with the PRK model instantiation method discussed in Section III-B, the above field-deployable signaling mechanisms enable agile, high-fidelity identification of interference relations between nodes, thus serving as a foundation for predictable interference control.

Remarks. For awareness of mutual interference relations, nodes exchange PRK model parameters and maintain local signal maps in the aforementioned protocol signaling method. The frequency of PRK model parameter exchange tends to be low compared with the frequency of data communications. For each link, in particular, one link reliability sample is collected only after every W number of data packets have been transmitted along the link, and a new link reliability sample may trigger one feedback-control update of the PRK model parameter and its sharing with nodes in the exclusion region. PRK model parameters can also be piggybacked into the data packets and control packets (e.g., those for maintaining local signal maps) that a node has to transmit anyway, thus further reducing the overhead of exchanging PRK model parameters.

For mostly-immobile wireless control networks which we consider in this study, the average wireless path loss usually does not change at short timescales (e.g., minutes or longer), thus the local signal maps can be maintained through infrequent packet exchanges between close-by nodes too. The control packets for signal map maintenance may be transmitted at a power level higher than data transmission powers should nodes beyond data communication ranges interfere with one another. As a first step towards ensuring predictable interference control in data transmission scheduling, our study here focuses on a single data transmission channel; when multiple data

transmission channels are used, the size of exclusion regions will significantly decrease [27], and the power level needed for signal map maintenance will significantly decrease too. To further reduce power consumption for signal map maintenance, approximate signal maps may be used such that power attenuation between nodes beyond data communication ranges may be estimated based on spatial channel correlations [28], [29] and power attenuation between nodes within data communication ranges. Detailed study of multi-channel scheduling and approximate signal maps, however, is beyond the scope of this paper, which focuses on the feasibility and basic mechanisms for ensuring predictable interference control in the presence of uncertainties in data transmission scheduling. The implementation and deployment of our approach in the NetEye [18] and Indriya [19] wireless network testbeds with resource-constrained TelosB motes, as we will discuss in Section IV, also demonstrate the feasibility of our approach in real-world wireless control networks whose nodes may well be less resource-constrained than TelosB (which only has a 8MHz processor and 10KB RAM).

D. Protocol PRKS: putting things together

Decoupling of protocol signaling & data transmission. Based on the methods of PRK model instantiation and protocol signaling presented in Sections III-B and III-C respectively, two basic tasks of interference control are 1) enabling nodes to be accurately aware of the mutual interference relations among themselves and 2) controlling channel access so that no two interfering links use the same wireless channel at the same time. These tasks make the commonly-used contention-based approach unsuitable for the following reasons:

- In contention-based channel access control, each data transmission is usually preceded by a protocol signaling phase either implicitly through carrier sensing or explicitly through RTS-CTS handshake such as in IEEE 802.11. Due to the probabilistic nature of wireless communication and the potentially large interference range, it is difficult to make such per-transmission protocol signaling perfectly reliable even with the mechanisms discussed in Section III-C. Accordingly, it is difficult for nodes to be accurately aware of their mutual interference relations, thus it is difficult to control interference in a predictable manner.
- Even if we can make the per-transmission protocol signaling more reliable through mechanisms such as retransmission of signaling packets, this introduces significant delay and overhead for each data transmission.

To address the aforementioned challenges, we propose to decouple protocol signaling from data transmission by leveraging the different timescales of PRK model adaptation and data transmission. Given a link (S, R), highly accurate estimation of its reliability usually requires the knowledge of the transmission status of several (e.g., 20) data transmissions along (S, R) [8]. Accordingly, it takes time to get a new link reliability feedback, and *the timescale of PRK model adaptation as well as the resulting change in interference relations between* (S, R) *and close-by nodes/links is longer than the timescale of individual data transmissions along* (S, R). Using the protocol signaling mechanisms discussed in Section III-C, the receiver R can inform, after each PRK model adaptation, the relevant nodes of the new value of parameter $K_{S,R,T_{S,R}}$ and thus the corresponding change in interference relations. Therefore, instead of requiring perfectly reliable signaling for each data transmission as in contention-based channel access control, we propose to treat protocol signaling as an independent process which ensures timely awareness of the mutual interference between nodes/links. Based on the latest information on mutual interference relations, data transmissions can be scheduled in a TDMA fashion without being coupled with protocol signaling.[7]

Besides enabling precise awareness of mutual interference relations between nodes/links, the decoupling of protocol signaling and data transmission also enables separating the transmission of signaling packets and data packets to prevent interference between protocol signaling and data transmission. Since protocol signaling does not introduce high traffic load and the timescale of PRK model adaptation as well as the resulting change in interference relations is longer than that of data packet transmission, we can separate protocol signaling and data transmission in time, for instance, by dedicating one time slot for transmitting signaling packets after every N (e.g., 20) time slots of data packet transmissions. In cases where there exists a control channel that has been set aside for control information exchange (e.g., in industry standards such as IEEE 1609.4 [30] and in research proposals [31], [32], [33]), we can also separate protocol signaling and data transmission in frequency by transmitting signaling packets in the control channel and data packets in the data channel. (We have experimented with both methods in our implementation and have observed similar scheduling performance; interested readers can find

[7]Note that the periodic sampling of physical processes in wireless control networks also makes TDMA an efficient scheduling mechanism as compared with contention-based approaches.

more implementation details in [12].)

Protocol PRKS. Based on the above design principles, we propose the PRK-based scheduling protocol *PRKS* that separates the functionalities of PRK-based channel access control into control plane functions and data plane functions as shown in Figure 2. In the control plane, the sender S and the receiver R of a given link (S, R) get to know the set of links whose transmissions cannot take place concurrently with the transmission from S to R through the protocol signaling mechanisms presented in Section III-C, and we define this set of links as the *conflict set* of link (S, R). More specifically, a link (C, D) is in the conflict set of (S, R) and thus conflicting with (S, R) at a time instant t if links (C, D) and (S, R) share a common end-node, $C \in \mathbb{E}_{S,R,T_{S,R}}(t)$, or $S \in \mathbb{E}_{C,D,T_{C,D}}(t)$, where $T_{S,R}$ and $T_{C,D}$ are the required packet delivery reliability across (S, R) and (C, D) respectively. Based on the conflict sets of links, data transmissions along individual links can be scheduled in a distributed, TDMA manner. In this study, we use the Optimal-Node-Activation-Multiple-Access (ONAMA) algorithm [34] which is a lightweight, distributed TDMA scheduling algorithm for wireless networks; we can also use other TDMA scheduling algorithms [35], but detailed study of TDMA scheduling itself is beyond the scope of this work. With the ONAMA algorithm, a link (S, R) is regarded as active in a time slot if S transmits to R in the slot. Given a time slot, the sender S first computes the priorities for (S, R) and the links in the conflict set of (S, R) to be active in the time slot, then S decides to transmit to R if and only if, for this time slot, (S, R) has higher priority to be active than every conflicting link. Every sender in the network computes link activation priorities in the same manner such that no two conflicting links will be active in the same time slot as long as the senders are accurately aware of their mutual interference relations. If a link (S, R) is active in a time slot, S transmits data packet(s) to R in this time slot. The statuses (i.e., successes or failures) of data transmissions in the data plane are fed back into the control plane for estimating the in-situ link reliabilities, which in turn triggers PRK model adaptation and then the adaptation of the TDMA transmission scheduling accordingly. In the control plane, nodes transmit signaling packets based on CSMA/CA since per-transmission reliability guarantee is not needed for signaling packets; nodes also leverage the transmissions and receptions of signaling packets to maintain their local signal maps as we have presented in Section III-C.

With the above approach to PRK-based scheduling, the TDMA scheduling of data transmissions happens at the beginning of each time slot based on the PRK model information that is readily available in the control plane, hence there is no need for ensuring perfectly reliable

protocol signaling on a per-transmission basis and thus no delay introduced on a per-transmission basis just for protocol signaling either. Given that the timescale of PRK model adaptation at a link (S, R) is longer than that of individual data transmissions along (S, R), in particular, the time instants t_a and t_b for two consecutive PRK model adaptations at (S, R) tend to be well separated such that, within the early part of the time window $[t_a, t_b]$, the PRK model parameter of link (S, R) generated at time t_a can be reliably delivered to the relevant nodes and then be used for the TDMA scheduling of data transmissions. In addition, we do not need perfect information consistency that requires the same PRK model parameter of a link (S, R) to be used by link (S, R) and all the links whose transmitters are in the exclusion region around receiver R. That is, a node can use the new PRK model parameter of a link the moment the node learns of the parameter. The intuition of this design is that the earliest use of new PRK model parameters helps improve data delivery reliability when the corresponding exclusion regions expand, or it helps improve the channel spatial reuse and the concurrency of data transmissions when the corresponding exclusion regions shrink. (Interested readers can find detailed discussions of this in [12].)

IV. Experimental evaluation

We have implemented PRKS in TinyOS [36], and we evaluate PRKS through measurement in the NetEye [18] and Indriya [19] wireless network testbeds.

A. Methodology

Protocols. To understand the design decisions of PRKS, we have comparatively studied PRKS with its variants; due to the limitation of space, however, we relegate the detailed discussions to [12]. Towards understanding the benefits of predictable interference control in PRKS, we implement in TinyOS the following distributed scheduling protocols and comparatively study their behavior with that of PRKS:

- *CSMA*: a contention-based MAC protocol that uses the basic CSMA/CA mechanism to ameliorate the impact of co-channel interference; this represents the interference control mechanism used by protocols such as B-MAC [25];
- *RTS-CTS*: a contention-based MAC protocol that uses CSMA/CA and RTS-CTS to ameliorate the impact of co-channel interference and hidden terminals; this represents the interference control mechanism used by protocols such as S-MAC [37];

- *RIDB*: a TDMA scheduling protocol that uses a TDMA protocol similar to the one used in PRKS and that uses the physical interference model to derive interference relations between nodes but ignores cumulative interference in networks [38].
- *CMAC*: a contention-based MAC protocol where a node transmits at a time instant only if the SINR of this transmission and the SINRs of other concurrent transmissions overheard by the node are above a certain threshold (e.g., for ensuring a certain link reliability); this represents the interference control mechanism used by protocols such as C-MAC [39];
- *SCREAM*: a TDMA scheduling protocol using the SCREAM primitive [16] to schedule concurrent transmissions according to the physical interference model; this represents the interference relation identification mechanism used by protocols such as FDD [16] and DSS [40].

Among these protocols, CSMA and RTS-CTS represent the protocol-model-based techniques in existing industry standards such as IEEE 802.15.4 and 802.11p; RIDB, CMAC, and SCREAM represent the techniques used in existing physical-model-based scheduling; similar to PRKS, RIDB and SCREAM also use the technique of separating TDMA-based data transmission from the control information exchange needed for generating the TDMA data transmission schedule. Focusing on predictable co-channel interference control, we do not compare PRKS with protocols such as WirelessHART [41] that do not consider channel spatial reuse.

Network and application settings. We use a subset of the 130 TelosB motes in NetEye by using each mote of NetEye with probability 0.8. Unless mentioned otherwise, every mote uses a data transmission power of -25dBm (i.e., power level 3 in TinyOS) such that a mote can only reach motes no more than 6 feet away with a packet delivery reliability (PDR) of over 95% in the absence of interference, thus forming a multi-hop network where not every mote can directly communicate with one another. Focusing on link-layer scheduling for predictable interference control in this study, we mainly consider one-hop data traffic where each mote transmits data packets to one of its neighboring motes to whom the PDR is above 95% in the absence of interference; if there are multiple such neighboring motes, each mote is selected as a receiver with equal probability. For understanding supportable network throughput while satisfying a certain application PDR requirement, we consider, unless mentioned otherwise, the saturated traffic scenario where every mote always has packets to transmit.

For reflecting different application scenarios, we consider the cases when the mean PDR requirement for each link are set to 70%, 80%, 90%, or 95% respectively. To understand

the adaptation of PRKS to online dynamics, we run experiments where the mean link-PDR requirement changes over time, for instance, setting the PDR requirement to 70%, 80%, 90%, 95%, 90%, 80%, and 70% over time.

We have experimented with other network and traffic conditions including in the Indriya [19] wireless network testbed and with heterogeneous PDR requirements, traffic load, and transmission power across different links, unsaturated and irregular traffic, temporally-varying traffic, as well as multi-hop traffic. We have observed similar phenomena as what we will present in Section IV-B. Interested readers can find the detailed discussions in [12].

B. Measurement results

Behavior of PRKS. For different PDR requirements, Figures 7 and 8 show the boxplots of link packet delivery reliability (PDR) and PRK model parameter in PRKS respectively. We see that PRKS adapts the PRK model parameter according to different PDR requirements, and that the required minimum mean PDR is always guaranteed in PRKS through predictable interference control.[8] In particular, the PRK model parameter increases with the PDR requirement so that more close-by nodes are prevented from transmitting concurrently with a link's transmission.

To understand the spatial reuse in PRKS, Figure 9 shows the mean concurrency (i.e., number of concurrent transmissions at a time instant) and its 95% confidence interval[9] in PRKS as well as in a state-of-the-art, centralized scheduling protocol *iOrder* [20] which maximizes channel spatial reuse in interference-oriented scheduling.[10] We see that, despite its nature of local and distributed control, PRKS enables a concurrency and spatial reuse statistically equal or close to what is enabled by the centralized algorithm iOrder while ensuring the required PDR at the same time.

Despite the distributed nature of the minimum-variance regulation controller in PRKS, the individual controllers converge to a state where the required PDR is satisfied. For a typical link in the network, for instance, Figure 10 shows the temporal behavior of link PDR when the

[8]Due to the discrete nature of the spatial distribution of concurrent transmitters, the actual PDR tends to be slightly higher than (instead of being strictly equal to) the required mean PDR.

[9]For the figures of this section that present performance statistics (e.g., mean concurrency or PDR), we also show the 95% confidence intervals of the statistics, but some of the confidence intervals may be too narrow to be noticeable in the figures.

[10]In terms of maximizing spatial reuse, iOrder has been shown to outperform well-known existing scheduling protocols such as Longest-Queue-First [42], GreedyPhysical [43], and LengthDiversity [44].

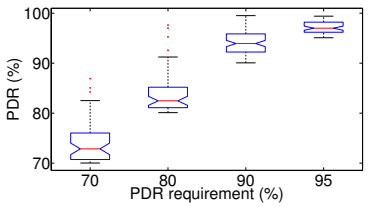

Fig. 7. Packet delivery reliability (PDR) in PRKS

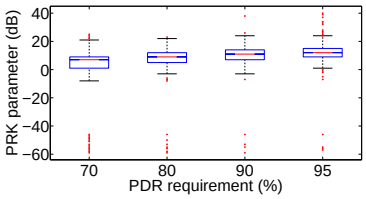

Fig. 8. PRK model parameter in PRKS

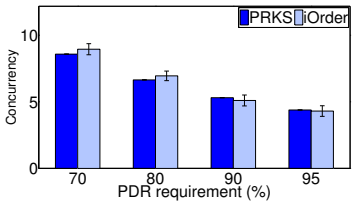

Fig. 9. Mean concurrency in PRKS and iOrder

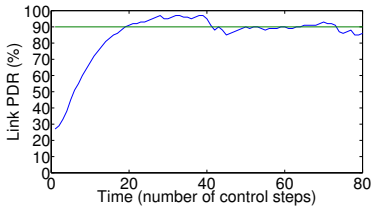

Fig. 10. Temporal link PDR: PDR req. = 90%

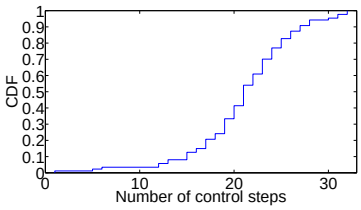

Fig. 11. CDF for the settling time of link PDR

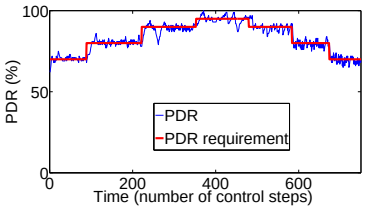

Fig. 12. PDR in PRKS: temporally varying PDR requirements

minimum application PDR requirement is 90%. We see that the link PDR converges to its steady state after around 25 control steps, where the PRK model parameter of the link is adapted once in each control step and each control step takes $\sim$100ms time. In general, link PDRs converge quickly, as shown by Figure 11 where the settling time is defined as the number of control steps taken for a link to reach its steady state PDR distribution. In addition to convergence to a state where the required PDRs are satisfied, the collective behavior of the distributed controllers in PRKS also enables a spatial reuse close to what is feasible with the state-of-the-art, centralized scheduler iOrder as we have shown in Figure 9.

For the adaptation of PRKS to online dynamics, Figure 12 shows, for a typical link in the network, the time series of link PDR when the application PDR requirement is set to 70%, 80%, 90%, 95%, 90%, 80%, and 70% over time. We see that, as the application PDR requirement varies, the link PDR adapts to meet the application requirement.

Comparison with existing protocols. Figure 13 shows the ratio of links whose PDRs are no less than the application required PDRs in PRKS and other existing protocols. We see that, unlike PRKS that always ensures application required PDRs for all the links in a predictable manner, existing protocols do not ensure the required PDRs due to co-channel interference that is not well controlled. We also see that the PDR satisfaction ratios in the existing protocols tend

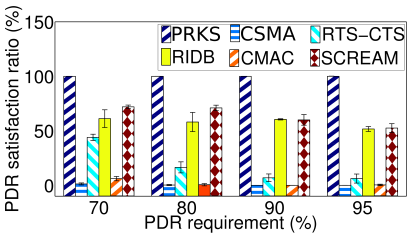

Fig. 13. PDR requirement satisfaction ratios in different protocols

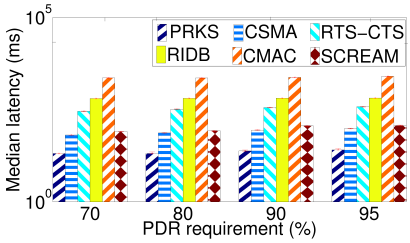

Fig. 14. Median latency: reliability via packet retransmission

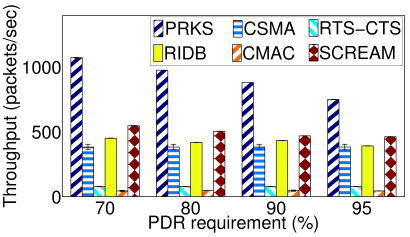

Fig. 15. Mean network spatial throughput

to decrease with increasing PDR requirements, thus the existing protocols cannot control link reliability in a predictable manner.

Among the existing protocols, RIDB enables higher PDR satisfaction ratios than RTS-CTS and CSMA do because RIDB considers the physical interference model and application PDR requirements in defining pairwise interference relations between nodes; nonetheless, due to its lack of consideration of cumulative interference from multiple concurrent interferers, RIDB does not ensure predictable interference control and thus does not ensure predictable link reliability. When the application PDR requirement is 95%, for instance, RIDB can only enable a PDR satisfaction ratio 50.72%. RTS-CTS ensures higher PDR satisfaction ratio than CSMA does due to its use of RTS-CTS handshake, but the PDR satisfaction ratios are quite low in both protocols (e.g., as low as 8.5% and 0% in RTS-CTS and CSMA respectively) since neither protocols are based on high-fidelity interference models.

Among the existing protocols that explicitly use the physical interference model, CMAC and SCREAM consider cumulative interference. Nonetheless, the PDR satisfaction ratio is quite low in CMAC, and the PDR satisfaction ratio in SCREAM can also be as low as 50%. CMAC cannot ensure the required PDRs since CMAC cannot ensure predictable interference control when the interference range is greater than the communication range, which is usually the case in practice (especially when the required PDR is high). Since CMAC does not decouple control signaling from data transmissions as in PRKS, interference control in CMAC is also negatively affected by any unreliability in the per-transmission-based control signaling (e.g., observing neighboring nodes' SINRs). In SCREAM, the collision among a set of concurrent transmitters is detected through network-wide coordination. The detection is based on a sample of the status (i.e., success or failure) of concurrent data transmissions and cannot ensure accurate collision detection, thus SCREAM cannot accurately control interference to ensure predictable PDR.

Incapable of ensuring predictable link reliability in scheduling, existing protocols can try to improve link reliability by packet retransmission. Nonetheless, packet retransmission increases data delivery latency; this can be seen from Figure 14 which shows the median packet delivery latency when packets are retransmitted to ensure a certain required PDR. Packet retransmission in existing protocols also reduces network throughput, as shown by Figure 15 which shows the mean number of data packets successfully delivered in the network per second.

Existing protocols can also try to improve link reliability by reducing the application traffic load such that interference becomes negligible. Nonetheless, this approach significantly decreases network throughput; this can be seen from Figure 16 which shows the mean network spatial throughput (i.e., number of data packets successfully delivered per second in the network) when data packet arrival rates are limited from above to ensure a certain required PDR.

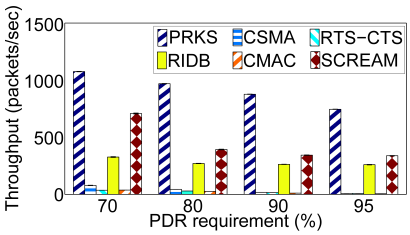

Fig. 16. Mean network throughput: reliability via traffic load reduction

Control message overhead. Table I shows the control message overhead in different protocols, where the overhead is defined as the ratio of the amount of control information exchange to that of data exchange in different protocols, W denotes the number of packet transmission status samples taken to generate a link reliability estimate in PRKS,[11] and L denotes the number of bytes of data in each data packet. In Table I, the term $o(t)$ denotes the type of control message overhead that is incurred at rather low frequency (as compared with the frequency of data packet exchange) and thus is negligible in the long-term; this includes the overhead incurred for signal map maintenance in PRKS and TDMA schedule generation in SCREAM. The overhead analysis in Table I assumes the following: it takes two bytes to encode a link PRK model parameter, two bits to encode link transmission status in ONAMA (which is used in PRKS), four bytes to encode the RTS and CTS messages in RTS-CTS and CMAC, and one byte to encode transmission power in CMAC.

Protocol	PRKS	CSMA	RTS-CTS	CMAC	SCREAM
Overhead	$\frac{W+8}{4WL} + o(t)$	0	$\frac{8}{L}$	$\frac{9}{L}$	$o(t)$

TABLE I
CONTROL MESSAGE OVERHEAD

CSMA does not introduce any control overhead since nodes do not explicitly exchange any

[11] $W = 20$ in our measurement study.

control information. The overhead in SCREAM is lower than that in PRKS since the TDMA schedule is updated at very low frequency in SCREAM. The overhead in RTS-CTS and CMAC is higher than that in PRKS because the RTS and CTS handshake is needed for every data transmission in RTS-CTS and CMAC. In PRKS, the limited control message exchange between close-by nodes enables nodes to be aware of their mutual interference relations; this enables predictable link reliability, which is a basis for mission-critical wireless networked control. As we have shown in Figures 14 and 15, predictable link reliability also enables significantly lower communication delay and higher data throughput, thus compensating for the overhead paid for the necessary control signaling. As we have discussed in Section III-C, the control overhead in PRKS can be further reduced (e.g., through approximate PRK models), but detailed study of this is beyond the scope of this paper.

V. Related work

Similar to PRKS, existing physical-model-based scheduling algorithms also try to control concurrent transmissions so that link reliabilities or receiver-side SINRs are above a certain threshold. Due to the non-local, combinatorial nature of the physical interference model, however, distributed physical-model-based scheduling algorithms have various drawbacks such as requiring network-wide coordination and employing strong systems assumptions which make it difficult to deploy these algorithms in real-world settings [6], [12].

Learning-based approaches have been taken to concurrently schedule throughput-improving exposed terminals [45], but those approaches did not ensure predictable link reliability since, similar to CMAC as discussed in Section IV, they only try to improve locally-observed throughput without ensuring predictable control of receiver-side cumulative interference. Learning-based approaches have also been taken to generate maximal sets of non-interfering transmitters [46], but they did not address the important question of how to identify the exclusion regions around receivers so that a required link reliability is guaranteed. The concepts of guard-zone or exclusion-region around receivers have also been exercised in distributed scheduling algorithms [47], [48], but these algorithms assumed uniform traffic load or uniform wireless signal power attenuation across the whole network, which are unrealistic in general.

Adaptive physical carrier sensing has been proposed to enhance network throughput [49], [50], but cumulative interference is not considered. We have also observed in [6] that throughput-optimal scheduling usually leads to low link reliability, which is not desirable in wireless

networked control. Park et al. [51] considered link reliability when adapting carrier sensing range, but their solution did not guarantee link reliability due to the price function involved. Fu et al. [52] proposed to control carrier sensing range to ensure a certain SINR at receivers, but the derivation of safe-carrier-sensing-range was based on the unrealistic assumption of homogeneous signal power attenuation across the whole network.

Scheduling via local coordination between close-by nodes has also been considered [43], [53], [10], [54]. Not focusing on distributed scheduling for predictable link reliability in real-world settings, however, these work assumed uniform wireless signal power attenuation which does not hold in practice in general [43], [53], [10], they did not consider the important question of how to identify the specific local region for inter-node coordination [54], [10], they focused on centralized scheduling [54], [43], or they focused on maximizing network throughput without considering predictable link reliability [53].

Focusing on addressing the open problem of predictable co-channel interference control in the presence of channel spatial reuse, our study in this paper does not consider frequency hopping for addressing external interference, duty-cycling for energy efficiency, real-time scheduling, other link-reliability control techniques such as rate adaptation and power control, or other interference management techniques such as interference cancellation, non-destructive interference, and multi-channel scheduling. The basic mechanisms of PRKS, however, are synergistic and can be integrated with the aforementioned techniques; due to the limitation of space, we relegate the detailed discussion to [12].

VI. Concluding remarks

To enable predictable reliability in data delivery for wireless networked control, we have proposed the wireless transmission scheduling protocol PRKS for predictable interference control in the presence of non-local interference as well as network and environmental uncertainties. Extensive experimental analysis shows that PRKS enables predictable link reliability while achieving a high degree of channel spatial reuse in data transmissions. Besides being important by itself, the predictable link reliability enabled by PRKS serves as a basis for predictable real-time data delivery and for predictable, controllable tradeoff between the reliability, delay, and throughput in wireless control networks; this enables predictable, controllable exploration of the network real-time capacity region, which in turn enables networking and control co-design in wireless networked control where the control system can pick the operating point

in the network real-time capacity region to optimize control performance. The predictable link reliability enabled by PRKS also represents a fundamental departure from the existing link-layer scheduling/MAC protocols which can only provide a best-effort communication service due to the lack of predictable interference control, and this has deep implications to the design of higher-layer protocols such as routing protocols. These topics of research are interesting future directions worth pursuing.

REFERENCES

[1] R. Z. (Editor), *Industrial Communication Technology Handbook*. CRC Press, 2015.

[2] J. R. Moyne and D. M. Tilbury, "Control and communication challenges in networked real-time systems," *Proceedings of the IEEE*, vol. 95, no. 1, pp. 9–28, 2007.

[3] X. Liu, H. Zhang, Q. Xiang, X. Che, and X. Ju, "Taming uncertainties in real-time routing for wireless networked sensing and control," *IEEE Transactions on Smart Grid (TSG)*, vol. 4, no. 1, 2012.

[4] J. R. Moyne and D. M. Tilbury, "The emergence of industrial control networks for manufacturing control, diagnostics, and safety data," *Proceedings of the IEEE*, vol. 95, no. 1, 2007.

[5] S. Srinivasa and M. Haenggi, "Throughput-delay-reliability tradeoffs in multihop networks with random access," in *Allerton Conference on Communication, Control, and Computing*, 2010.

[6] H. Zhang, X. Che, X. Liu, and X. Ju, "Adaptive instantiation of the protocol interference model in wireless networked sensing and control," *ACM Transactions on Sensor Networks (TOSN)*, vol. 10, no. 2, 2014.

[7] H. Zhang, A. Arora, Y. ri Choi, and M. Gouda, "Reliable bursty convergecast in wireless sensor networks," *Computer Communications (Elsevier)*, vol. 30, no. 13, 2007.

[8] H. Zhang, A. Arora, and P. Sinha, "Link estimation and routing in sensor network backbones: Beacon-based or data-driven?" *IEEE Transactions on Mobile Computing*, vol. 8, no. 5, pp. 653 – 667, May 2009.

[9] R. Maheshwari, S. Jain, and S. Das, "A measurement study of interference modeling and scheduling in low-power wireless networks," in *ACM SenSys*, 2008.

[10] B. Katz, M. Volker, and D. Wagner, "Link scheduling in local interference models," in *AlgoSensors*, 2008.

[11] H. Zhang, C. Li, X. Liu, Y. Chen, X. Che, F. Lin, L. Y. Wang, and G. Yin, "Scheduling with predictable link reliability for wireless networked control," in *IEEE/ACM IWQoS*, 2015.

[12] ——, "Scheduling with predictable link reliability for wireless networked control," Wayne State University, Tech. Rep. DNC-TR-16-02 (https://sites.google.com/site/dnctrs/DNC-TR-16-02.pdf), 2016.

[13] A. Saifullah, D. Gunatilaka, P. Tiwari, M. Sha, C. Lu, B. Li, C. Wu, and Y. Chen, "Schedulability Analysis under Graph Routing in WirelessHART Networks," in *IEEE RTSS*, 2015.

[14] M. Pajic, S. Sundaram, G. J. Pappas, and R. Mangharam, "The wireless control network: A new approach for control over networks," *IEEE Transactions on Automatic Control*, vol. 56, no. 10, pp. 2305–2318, 2011.

[15] Y. Yi, G. D. Veciana, and S. Shakkottai, "On optimal MAC scheduling with physical interference model," in *IEEE INFOCOM*, 2007.

[16] G. Brar, D. M. Blough, and P. Santi, "The SCREAM approach for efficient distributed scheduling with physical interference in wireless mesh networks," in *ICDCS*, 2008.

[17] A. H. Mohsenian-Rad, V. W. Wong, and R. Schober, "Optimal SINR-based random access," in *IEEE INFOCOM*, 2010.

[18] X. Ju, H. Zhang, and D. Sakamuri, "NetEye: A user-centered wireless sensor network testbed for high-fidelity, robust experimentation," *International Journal of Communication Systems (Wiley)*, vol. 25, no. 9, pp. 1213–1229, 2012.

[19] M. Doddavenkatappa, M. C. Chan, and A. L. Ananda, *Testbeds and Research Infrastructure: Development of Networks and Communities*. Springer, 2012, ch. Indriya: A Low-Cost, 3D Wireless Sensor Network Testbed.

[20] X. Che, H. Zhang, and X. Ju, "The case for addressing the ordering effect in interference-limited wireless scheduling," *IEEE Transactions on Wireless Communications*, vol. 13, no. 9, 2014.

[21] A. Cerpa, J. Wong, M. Potkonjak, and D. Estrin, "Temporal properties of low power wireless links: Modeling and implications on multi-hop routing," in *ACM MobiHoc*, 2005.

[22] J. Hellerstein, Y. Diao, S. Parekh, and D. M. Tilbury, *Feedback Control of Computing Systems*. Wiley-IEEE Press, 2004.

[23] X. Chang, J. Huang, S. Liu, G. Xing, H. Zhang, J. Wang, L. Huang, and Y. Zhuang, "Accuracy-aware interference modeling and measurement in wireless sensor networks," *IEEE Transactions on Mobile Computing*, vol. 15, no. 2, 2016.

[24] MEMSIC, INC, "TelosB sensor node," http://www.memsic.com, 2015.

[25] J. Polastre, J. Hill, and D. Culler, "Versatile low power media access for wireless sensor networks," in *ACM SenSys*, 2004.

[26] B. Williams and T. Camp, "Comparison of Broadcasting Techniques for Mobile Ad Hoc Networks," in *ACM MobiHoc*, 2002.

[27] X. Che and H. Zhang, "PRK Interference Model in Multi-Channel Wireless Networks," Wayne State University, Tech. Rep. DNC-TR-14-04 (https://sites.google.com/site/dnctrs/DNC-TR-14-04.pdf), 2014.

[28] Y. Xu and W. chien Lee, "Exploring spatial correlation for link quality estimation in wireless sensor networks," in *IEEE PERCOM*, 2006.

[29] P. Agrawal and N. Patwari, "Correlated link shadow fading in multi-hop wireless networks," *IEEE Transactions on Wireless Communication*, vol. 8, no. 8, pp. 4024–4036, 2009.

[30] IEEE 1609.4, "IEEE standard for wireless access in vehicular environments (WAVE) — multi-channel operation," IEEE Std 1609.4, 2010.

[31] J. So and N. Vaidya, "Multi-channel MAC for ad hoc networks: Handling multi-channel hidden terminals using a single transceiver," in *ACM MobiHoc*, 2004.

[32] S.-L. Wu, C.-Y. Lin, Y.-C. Tseng, and J.-L. Sheu, "A new multi-channel MAC protocol with on-demand channel assignment for multi-hop mobile ad hoc networks," in *IEEE ISPAN*, 2000.

[33] S. Park and S.-M. Yoo, "An efficient reliable one-hop broadcast in mobile ad hoc networks," *Ad Hoc Networks*, vol. 11, no. 1, pp. 19–28, 2013.

[34] X. Liu, Y. Chen, and H. Zhang, "A maximal concurrency and low latency distributed scheduling protocol for wireless sensor networks," *International Journal of Distributed Sensor Networks (Hindawi)*, no. 603172, 2015.

[35] J.-H. Ju and V. O. K. Li, "An optimal topology-transparent scheduling method in multihop packet radio networks," *IEEE/ACM Transactions on Networking*, vol. 6, no. 3, pp. 298–306, 1998.

[36] P. Levis, S. Madden, J. Polastre, R. Szewczyk, K. Whitehouse, A. Woo, D. Gay, J. Hill, M. Welsh, E. Brewer, and D. Culler, *Ambient Intelligence*. Springer, 2005, ch. TinyOS: An Operating System for Sensor Networks.

[37] W. Ye, J. Heidemann, and D. Estrin, "An energy-efficient MAC protocol for wireless sensor networks," in *IEEE InfoCom*, 2002, pp. 1567–1576.

[38] G. Zhou, T. He, J. A. Stankovic, and T. Abdelzaher, "RID: Radio interference detection in wireless sensor networks," in *IEEE INFOCOM*, 2005.

[39] M. Sha, G. Xing, G. Zhou, S. Liu, and X. Wang, "C-MAC: Model-driven concurrent medium access control for wireless sensor networks," in *IEEE INFOCOM*, 2009.

[40] J. Ryu, C. Joo, T. Kwon, N. Shroff, and Y. Choi, "DSS : Distributed SINR-based scheduling algorithm for multihop wireless networks," *IEEE Transactions on Mobile Computing*, vol. 12, no. 6, pp. 1120–1132, 2013.

[41] D. Chen, M. Nixon, and A. Mok, *Wireless*HART*: Real-Time Mesh Network for Industrial Automation*. Springer, 2010.

[42] L. B. Le, E. Modiano, C. Joo, and N. B. Shroff, "Longest-queue-first scheduling under SINR interference model," in *ACM MobiHoc*, 2010.

[43] G. Brar, D. M. Blough, and P. Santi, "Computationally efficient scheduling with the physical interference model for throughput improvement in wireless mesh networks," in *ACM MobiCom*, 2006.

[44] O. Goussevskaia, Y. A. Oswald, and R. Wattenhofer, "Complexity in geometric SINR," in *ACM MobiHoc*, 2007.

[45] M. Vutukuru, K. Jamieson, and H. Balakrishnan, "Harnessing exposed terminals in wireless networks," in *NSDI*, 2008.

[46] M. Durvy and P. Thiran, "Reaction-diffusion based transmission patterns for ad hoc networks," in *IEEE INFOCOM*, 2005.

[47] L. X. Cai, L. Cai, X. Shen, J. W. Mark, and Q. Zhang, "MAC protocol design and optimization for multi-hop ultra-wideband networks," *IEEE TWC*, vol. 8, no. 8, 2009.

[48] A. Hasan and J. G. Andrews, "The guard zone in wireless ad hoc networks," *IEEE TWC*, vol. 6, no. 3, 2007.

[49] L. B. Jiang and S. C. Liew, "Improving throughput and fairness by reducing exposed and hidden nodes in 802.11 networks," *IEEE Transactions on Mobile Computing*, vol. 7, no. 1, 2006.

[50] H. Ma, H. M. Alazemi, and S. Roy, "A stochastic model for optimizing physical carrier sensing and spatial reuse in wireless ad hoc networks," in *IEEE MASS*, 2005.

[51] K.-J. Park, L. Kim, and J. C. Hou, "Adaptive physical carrier sense in topology-controlled wireless networks," *IEEE Transactions on Mobile Computing*, vol. 9, no. 1, 2009.

[52] L. Fu, S. C. Liew, and J. Huang, "Effective carrier sensing in CSMA networks under cumulative interference," in *IEEE INFOCOM*, 2010.

[53] Y. Xu and W. Wang, "Scheduling partition for order optimal capacity in large-scale wireless networks," *IEEE Transactions on Mobile Computing*, vol. 12, no. 4, pp. 666–679, 2013.

[54] L. Badia, A. Erta, L. Lenzini, F. Rossetto, and M. Zorzi, "A physical model scheduler for multi-hop wireless networks based on local information," in *IEEE MASS*, 2008.